
Higher-dimensional deterministic formulation of hyperbolic conservation laws with uncertain initial data

Michael Herty, Adrian Kolb and Siegfried Müller

Institut für Geometrie und Praktische Mathematik
Templergraben 55, 52062 Aachen, Germany

M. Herty

Institut für Geometrie und Praktische Mathematik, RWTH Aachen University, Templergraben 55, D-52056 Aachen, Germany

E-mail: herty@igpm.rwth-aachen.de

A. Kolb

Institut für Geometrie und Praktische Mathematik, RWTH Aachen University, Templergraben 55, D-52056 Aachen, Germany

E-mail: kolb@eddy.rwth-aachen.de

S. Müller

Institut für Geometrie und Praktische Mathematik, RWTH Aachen University, Templergraben 55, D-52056 Aachen, Germany

E-mail: mueller@igpm.rwth-aachen.de

Higher-dimensional deterministic formulation of hyperbolic conservation laws with uncertain initial data

M. Herty · A. Kolb · S. Müller

Abstract We discuss random hyperbolic conservation laws and introduce a formulation interpreting the stochastic variables as additional spatial dimensions with zero flux. The approach is compared with established non-intrusive approaches to random conservation laws. In the scalar case, an entropy solution is proven to exist if and only if a random entropy solution for the original problem exists. Furthermore, existence and numerical convergence of stochastic moments is established. Along with this, the boundedness of the L^1 -error of the stochastic moments by the L^1 -error of the approximation is proven. For the numerical approximation a Runge–Kutta discontinuous Galerkin method is employed and a multi-element stochastic collocation is used for the approximation of the stochastic moments. By means of grid adaptation the computational effort is reduced in the spatial as well as in the stochastic directions, simultaneously. Results on Burgers' and Euler equation are validated by several numerical examples and compared to Monte Carlo simulations.

Keywords Hyperbolic conservation laws · uncertainty quantification · discontinuous Galerkin methods · stochastic collocation · multiresolution analysis

Mathematics Subject Classification (2000) 65M50, 35L65, 65N30, 65M70

1 Introduction

In the past decades accurate and stable schemes for hyperbolic systems of conservation laws have been subject to intensive research and there has been tremendous progress towards reliable and efficient schemes leading in turn to a number of applications even outside classical gas dynamics. However, in practical applications measurement errors usually have to be taken into account and hence, the deterministic nature of the formulation changes. Those errors might be modeled as stochastic uncertainties in the input and are usually treated within a probabilistic framework. Moreover, epistemic uncertainties arise, when the considered mathematical models do not exactly describe the true physical reality. When the underlying model is not known exactly, but is given by a probability law or by statistical moments, the deterministic case is extended to the stochastic case.

M. Herty

Institut für Geometrie und Praktische Mathematik, RWTH Aachen University, Templergraben 55, D-52056 Aachen, Germany

E-mail: herty@igpm.rwth-aachen.de

A. Kolb

Institut für Geometrie und Praktische Mathematik, RWTH Aachen University, Templergraben 55, D-52056 Aachen, Germany

E-mail: kolb@eddy.rwth-aachen.de

S. Müller

Institut für Geometrie und Praktische Mathematik, RWTH Aachen University, Templergraben 55, D-52056 Aachen, Germany

E-mail: mueller@igpm.rwth-aachen.de

Several approaches have been proposed in the past to deal with the stochastic case both from an analytical and numerical perspective. A broad classification distinguishes non-intrusive and intrusive methods. Among the non-intrusive methods, the Monte Carlo method and its variants, apply a deterministic concept to each realization. Such sampling-based methods in the context of hyperbolic equations are used e.g. in [20, 19, 1]. An intrusive approach on the contrary uses the representation of stochastic perturbations by a series of orthogonal functions, known as generalized polynomial chaos (or -Loève) expansions [3, 34]. Those expansions are substituted in the governing hyperbolic equations and projected on a (finite dimensional) subspace. This leads to deterministic evolution equations for the coefficients of the series expansion. In particular, in the context of partial differential equations this has been applied successfully for a large class of problems and we refer to e.g. [9, 3, 12, 14, 25, 35] and references therein for some examples. In the context of hyperbolic problems there have been many recent contributions in particular based on the observation that the projected deterministic system might encounter a loss of hyperbolicity.

Besides the theoretical obstacles of the intrusive or non-intrusive approaches, several contributions towards numerical schemes and their convergence analysis have been proposed and we refer to [20, 19, 10, 24, 22, 6] for further reference.

In stochastic problems the main interest is in some averaged quantities such as expectation and variance. However, the computation of stochastic quantities for instance using Monte Carlo methods is very time-consuming due to low convergence rates requiring a large number of samples. In the context of conservation laws known to exhibit discontinuities in space the convergence behavior is even worse because discontinuities may also be present in the stochastic variables. Thus, to improve efficiency we suggest a new strategy for the computations of the stochastic moments that allows for local refinement in the spatial domain as well as in the stochastic domain. For this purpose, we introduce the stochastic variables as additional “spatial” variables. This will make the resulting problem higher-dimensional but deterministic. This idea of parameterizing the stochastic variables has already been studied in [26, 30], where a path-wise solution of the probabilistic shock profile was used. There the equivalence of the stochastic solution and the parameterized solution is not proven. We generalize these results and describe a numerical approach that takes into account the local stochastic structure. The additional effort of the higher dimensional problem is compensated for by local grid adaptation and multi-element stochastic collocation methods allowing for a more efficient computation of stochastic quantities.

The outline of the paper is as follows: First of all, we introduce the stochastic Cauchy problem and summarize well-known results for the entropy solution from [20], see Section 2. In Section 3 we propose a method based on embedding the stochastic problem in a higher-dimensional space resulting in a deterministic problem in the spatial and stochastic variables. We verify that the entropy solutions of the stochastic Cauchy problem and the deterministic Cauchy problem coincide. This holds true for a class of absolutely continuous random variables. Existence of statistical moments of the solution is obtained by modifications of classical results. In Section 4 we outline the numerical discretization and convergence of the discrete statistical moments. Finally, numerical comparisons with non-intrusive methods are presented in Section 5 for Burgers’ equation as well as the Euler equations with a single random variable.

2 The scalar stochastic Cauchy problem

In this section we introduce scalar conservation laws with uncertain initial data. For this purpose, we follow [20] and briefly summarize well-posedness of a random entropy solution and its stochastic moments. In contrast to [20], we will confine ourselves to absolutely continuous random variables.

Starting point is the probability space $(\Omega, \mathcal{F}, \mathbb{P})$ with Ω a non-empty set, \mathcal{F} a σ -algebra over Ω and \mathbb{P} a probability measure on \mathcal{F} . Let be $\xi : \Omega \rightarrow \Omega_\xi$ a random variable on $(\Omega, \mathcal{F}, \mathbb{P})$ and let be $\mathcal{F}_\xi := \mathcal{B}(\Omega_\xi)$ the Borel σ -algebra over $\Omega_\xi := \mathbb{R}^m$. For $B \in \mathcal{B}(\mathbb{R}^m)$ we define the probability distribution of ξ by $\mathbb{P}_\xi(B) \equiv \mathbb{P}(\xi^{-1}(B)) := \mathbb{P}(\{\omega \in \Omega : \xi(\omega) \in B\})$ on $(\mathbb{R}^m, \mathcal{B}(\mathbb{R}^m))$.

We assume that the probability distribution of ξ is an absolutely continuous random variable with respect to the Lebesgue measure. Then [2, Theorem 17.10] yields existence of an essentially bounded

density $p_\xi : \mathbb{R}^m \rightarrow [0, \infty)$ such that $\mathbb{P}_\xi(B) = \int_B p_\xi(\xi) d\xi$ for all $B \in \mathcal{B}(\mathbb{R}^m)$ and $\int_{\mathbb{R}^m} p_\xi(\xi) d\xi = 1$. Furthermore, we introduce stochastic quantities such as the expectation for a function $u \in L^1(\mathbb{R}^m)$ as

$$\mathbb{E}[u(\xi)] := \int_{\Omega} u(\xi(\omega)) d\mathbb{P}(\omega) = \int_{\mathbb{R}^m} u(\xi) p_\xi(\xi) d\xi \quad (1)$$

and its k -th centralized moments

$$\mathcal{M}_c^k[u(\xi)] := \mathbb{E}[(u(\xi) - \mathbb{E}[u(\xi)])^k], \quad k \in \mathbb{N}. \quad (2)$$

In particular, for $k = 2$ we obtain the variance

$$\text{Var}[u(\xi)] := \mathcal{M}_c^2[u(\xi)] = \mathbb{E}[(u(\xi) - \mathbb{E}[u(\xi)])^2]. \quad (3)$$

The random variable ξ is used in the stochastic Cauchy problem for scalar conservation laws

$$\bar{u}_t(t, x; \omega_\xi) + \sum_{j=1}^d \frac{\partial}{\partial x_j} f_j(\bar{u}(t, x; \omega_\xi)) = 0, \quad x \in \mathbb{R}^d, \omega_\xi \in \Omega_\xi, t \in (0, T) \quad (4a)$$

$$\bar{u}(0, x; \omega_\xi) = \bar{u}_0(x; \omega_\xi), \quad x \in \mathbb{R}^d, \omega_\xi \in \Omega_\xi. \quad (4b)$$

Here, $\bar{u}(t, x; \omega_\xi) \in \mathbb{R}$ is the conserved variable, $f \in C^1(\mathbb{R}, \mathbb{R}^d)$ is the flux field and $T \in (0, \infty)$ is the final time. Uncertainty enters the problem explicitly in the initial condition (4b). As in [20], we assume that the initial condition (4b) is given by an $L^1(\mathbb{R}^d)$ -valued random variable.

In analogy to the deterministic case [11], we define the entropy solution to the stochastic problem (4).

Definition 1 ([20], Definition 3.2) A random field $\bar{u} : \Omega_\xi \rightarrow C([0, T]; L^1(\mathbb{R}^d))$ is said to be a random entropy solution if it satisfies the following two conditions:

(i) Weak solution: For \mathbb{P}_ξ -a.s. $\omega_\xi \in \Omega_\xi$, $\bar{u}(\cdot, \cdot; \omega_\xi)$ satisfies the weak formulation

$$\begin{aligned} \int_0^\infty \int_{\mathbb{R}^d} \left(\bar{u}(t, x; \omega_\xi) \bar{\varphi}_t(t, x) + \sum_{j=1}^d f_j(\bar{u}(t, x; \omega_\xi)) \frac{\partial}{\partial x_j} \bar{\varphi}(t, x) \right) dx dt \\ + \int_{\mathbb{R}^d} \bar{u}_0(x; \omega_\xi) \bar{\varphi}(0, x) dx = 0 \end{aligned} \quad (5)$$

for all test functions $\bar{\varphi} \in C_0^1([0, T] \times \mathbb{R}^d)$.

(ii) Entropy condition: Let (η, Q) be an entropy–entropy flux pair, i.e., $\eta : \mathbb{R} \rightarrow \mathbb{R}$ is a convex function and $Q : \mathbb{R} \rightarrow \mathbb{R}^d$ with $Q'_j(\bar{u}) = \eta'(\bar{u}) f'_j(\bar{u})$, $j = 1, \dots, d$ for \mathbb{P}_ξ -a.s. $\omega_\xi \in \Omega_\xi$. Then, \bar{u} satisfies the inequality

$$\begin{aligned} \int_0^\infty \int_{\mathbb{R}^d} \left(\eta(\bar{u}(t, x; \omega_\xi)) \bar{\varphi}_t(t, x) + \sum_{j=1}^d Q_j(\bar{u}(t, x; \omega_\xi)) \frac{\partial}{\partial x_j} \bar{\varphi}(t, x) \right) dx dt \\ + \int_{\mathbb{R}^d} \eta(\bar{u}_0(x; \omega_\xi)) \bar{\varphi}(0, x) dx \geq 0 \end{aligned} \quad (6)$$

for all test functions $\bar{\varphi} \in C_0^1([0, T] \times \mathbb{R}^d)$ with $\bar{\varphi} \geq 0$.

In [20] it is proven that there exists a unique random entropy solution for a general probability space $(\Omega, \mathcal{F}, \mathbb{P})$, if the entropy solution exists for \mathbb{P} -a.s. $\omega \in \Omega$. Here, we restrict this results to the induced probability measure \mathbb{P}_ξ :

Theorem 1 ([20], Theorem 3.3) Consider the stochastic Cauchy problem (4a) with random initial data (4b) given by an $L^1(\mathbb{R}^d)$ -valued random variable \bar{u}_0 satisfying

$$\bar{u}_0(\cdot; \omega_\xi) \in (L^\infty \cap BV)(\mathbb{R}^d) \quad \text{for } \mathbb{P}_\xi\text{-a.s. } \omega_\xi \in \Omega_\xi. \quad (7)$$

Furthermore, we assume $\|\bar{u}_0\|_{L^k(\Omega_\xi; L^1(\mathbb{R}^d))} < \infty$ for some $k \in \mathbb{N}$. Then, there exists a unique random entropy solution $\bar{u} : \Omega_\xi \rightarrow C([0, T]; L^1(\mathbb{R}^d))$ such that for all $0 \leq t \leq T$ and all $k \in \mathbb{N}$:

$$\|\bar{u}\|_{L^k(\Omega_\xi; C([0, T]; L^1(\mathbb{R}^d)))} \leq \|\bar{u}_0\|_{L^k(\Omega_\xi; L^1(\mathbb{R}^d))}$$

and

$$\|\bar{u}(t, \cdot; \omega_\xi)\|_{(L^1 \cap L^\infty)(\mathbb{R}^d)} \leq \|\bar{u}_0(\cdot; \omega_\xi)\|_{(L^1 \cap L^\infty)(\mathbb{R}^d)}$$

for \mathbb{P}_ξ -a.s. $\omega_\xi \in \Omega_\xi$.

This theorem ensures well-posedness of a random entropy solution. Furthermore, if the k -th stochastic moment of the initial condition (4b) exists for some $k \in \mathbb{N}$, we obtain existence of the k -th moment of the random entropy solution. The definition can be extended to the system case.

3 Deterministic approach

Motivated by [26, 30] we introduce a deterministic approach to treat the stochastic parameter ω_ξ in a stochastic Cauchy problem. According to Section 2, there exists a random entropy solution, if the solution is a weak solution (5) and fulfills the entropy condition (6) for \mathbb{P}_ξ -a.s. $\omega_\xi \in \Omega_\xi$. This motivates to introduce the stochastic variables ω_ξ as additional (spatial) variables resulting in a deterministic problem in higher dimensions.

3.1 Formulation of the deterministic approach

In the sequel, we impose the following additional assumption on $\xi : \Omega \rightarrow \Omega_\xi$.

Hypothesis 1 Let be $V \subset \mathbb{R}^m$ an open bounded set with positive measure. Furthermore, let be $p_\xi : \mathbb{R}^m \rightarrow [0, \infty)$ the density of ξ and $p_U : V \rightarrow [0, \infty)$ the density to the uniform distribution $\mathcal{U}(V)$. Then, there exists a diffeomorphism $\Psi : V \rightarrow \mathbb{R}^m$ such that

$$p_\xi(\xi) = p_U(\Psi^{-1}(\xi)) |\det(D_\xi \Psi^{-1})(\xi)| = \frac{\chi_V(\Psi^{-1}(\xi))}{|V|} |\det(D_\xi \Psi^{-1})(\xi)| \neq 0. \quad (8)$$

Hypothesis 1 guarantees the existence of a transformation of the random variable ξ into a uniform random variable \mathcal{U} . Further information on such a transformation can be found, for example, in [15].

For $x \in \mathbb{R}^d$ and $\xi \in \mathbb{R}^m$ we introduce the new variable $y := (x, \xi) \in \mathbb{R}^{d+m}$. Furthermore, we define a new flux $f \in C^1(\mathbb{R}, \mathbb{R}^{d+m})$ with zero flux in the (stochastic) directions, i.e.,

$$f_{d+j} \equiv 0, \quad j = 1, \dots, m. \quad (9)$$

This leads to the following deterministic formulation

$$u_t(t, y) + \sum_{j=1}^{d+m} \frac{\partial}{\partial y_j} f_j(u(t, y)) = 0, \quad y \in \mathbb{R}^{d+m}, \quad t \in (0, T) \quad (10a)$$

$$u(0, y) = u_0(y), \quad y \in \mathbb{R}^{d+m}, \quad (10b)$$

with the new conserved variable $u(t, y) \equiv u(t, (x, \xi))$. Following the classical theory of deterministic scalar conservation laws, cf. [11], the entropy solution is then defined as follows:

Definition 2 A solution u to the deterministic Cauchy problem (10) is an entropy solution if it satisfies the following:

(i) Weak solution: u satisfies the weak formulation

$$\int_0^\infty \int_{\mathbb{R}^{d+m}} \left(u(t, y) \varphi_t(t, y) + \sum_{j=1}^{d+m} f_j(u(t, y)) \frac{\partial}{\partial y_j} \varphi(t, y) \right) dy dt + \int_{\mathbb{R}^{d+m}} u_0(y) \varphi(0, y) dy = 0 \quad (11)$$

for all test functions $\varphi \in C_0^1([0, T] \times \mathbb{R}^{d+m})$.

(ii) Entropy condition: Let (η, Q) be an entropy–entropy flux pair, i.e., $\eta : \mathbb{R} \rightarrow \mathbb{R}$ is a convex function and $Q : \mathbb{R} \rightarrow \mathbb{R}^{d+m}$ with $Q'_j(u) = \eta'(u) f'_j(u)$, $j = 1, \dots, d+m$. Then, u satisfies

$$\int_0^\infty \int_{\mathbb{R}^{d+m}} \left(\eta(u(t, y)) \varphi_t(t, y) + \sum_{j=1}^{d+m} Q_j(u(t, y)) \frac{\partial}{\partial y_j} \varphi(t, y) \right) dy dt + \int_{\mathbb{R}^{d+m}} \eta(u_0(y)) \varphi(0, y) dy \geq 0 \quad (12)$$

for all test functions $\varphi \in C_0^1([0, T] \times \mathbb{R}^{d+m})$ with $\varphi \geq 0$.

Some remarks are in order. Since there is zero flux in the stochastic directions we conclude from the compatibility condition for the entropy fluxes in the stochastic directions

$$Q'_{d+j} = 0, \text{ i.e., } Q_{d+j} = c_{d+j}, \quad j = 1, \dots, m \quad (13)$$

with $c_{d+j} \in \mathbb{R}$ for $j = 1, \dots, m$. According to [11, Chapter 2, Theorem 5.1, Theorem 5.2] the deterministic Cauchy problem (10) has a unique entropy solution $u(t, \cdot) \in (L^1 \cap L^\infty)(\mathbb{R}^{d+m})$ satisfying the maximum principle

$$\|u(t, \cdot)\|_{L^1(\mathbb{R}^{d+m})} \leq \|u_0\|_{L^1(\mathbb{R}^{d+m})}, \quad \|u(t, \cdot)\|_{L^\infty(\mathbb{R}^{d+m})} \leq \|u_0\|_{L^\infty(\mathbb{R}^{d+m})} \quad (14)$$

for all $t \in [0, T]$ provided $u_0 \in (L^1 \cap L^\infty)(\mathbb{R}^{d+m})$.

To justify our approach, we verify that the entropy solution of (10) coincides with the entropy solution in the sense of Definition 1.

Theorem 2 Assume (8) holds. Let \bar{u}_0 be a $L^1(\mathbb{R}^d)$ -valued random variable fulfilling (7) and let $u_0 \in (L^1 \cap L^\infty)(\mathbb{R}^{d+m})$ be the initial data of the deterministic problem (10) such that

$$u_0((x, \omega_\xi)) = \bar{u}_0(x; \omega_\xi) \quad \text{for } \mathbb{P}_\xi\text{-a.s. } \omega_\xi \in \Omega_\xi \quad \text{and for a.e. } x \in \mathbb{R}^d. \quad (15)$$

Furthermore, we assume that the flux fulfills (9). Then the stochastic Cauchy problem (4) has a unique entropy solution \bar{u} in the sense of Definition 1 if and only if there exists an entropy solution u in the sense of Definition 2. Furthermore it holds

$$u(t, (x, \omega_\xi)) = \bar{u}(t, x; \omega_\xi) \quad \text{for } \mathbb{P}_\xi\text{-a.s. } \omega_\xi \in \Omega_\xi \quad \text{and for a.e. } x \in \mathbb{R}^d. \quad (16)$$

Proof Let \bar{u} be according to Theorem 1. Let $\varphi \in C_0^1([0, T] \times \mathbb{R}^{d+m})$ be a test function. Then for $\omega_\xi \in \Omega_\xi$ fixed the restriction

$$\bar{\varphi}(t, x; \omega_\xi) := \varphi(t, (x, \omega_\xi)) \chi_V(\Psi^{-1}(\omega_\xi)) |V| / |\det(D_\xi \Psi^{-1})(\omega_\xi)| \quad (17)$$

is a test function in $C_0^1([0, T] \times \mathbb{R}^d)$ and the weak formulation (5) holds for \mathbb{P}_ξ -a.s. $\omega_\xi \in \Omega_\xi$. Integration of (5) over the induced probability space leads to

$$\begin{aligned} \int_{\Omega_\xi} \left(\int_0^\infty \int_{\mathbb{R}^d} \bar{u}(t, x; \omega_\xi) \bar{\varphi}_t(t, x; \omega_\xi) + \sum_{j=1}^d f_j(\bar{u}(t, x; \omega_\xi)) \frac{\partial}{\partial x_j} \bar{\varphi}(t, x; \omega_\xi) dx dt \right. \\ \left. + \int_{\mathbb{R}^d} \bar{u}_0(x; \omega_\xi) \bar{\varphi}(0, x; \omega_\xi) dx \right) d\mathbb{P}_\xi(\omega_\xi) = 0. \end{aligned} \quad (18)$$

Let us define $u(t, x, \omega_\xi) := \bar{u}(t, x; \omega_\xi)$ for \mathbb{P}_ξ -a.s. $\omega_\xi \in \Omega_\xi$ and for a.e. $x \in \mathbb{R}^d$. We will show that this is a weak solution for the formulation (11). Using (15), (17) and (9) this is equivalent to

$$\begin{aligned} \int_{\mathbb{R}^m} \left(\int_0^\infty \int_{\mathbb{R}^d} u(t, x, \xi) \varphi_t(t, x, \xi) + \sum_{j=1}^{d+m} f_j(u(t, x, \xi)) \frac{\partial}{\partial x_j} \varphi(t, x, \xi) dx dt \right. \\ \left. + \int_{\mathbb{R}^d} u_0(x, \xi) \varphi(0, x, \xi) dx \right) p_\xi(\xi) \chi_V(\Psi^{-1}(\xi)) |V| |\det(D_\xi \Psi^{-1})(\xi)| d\xi = 0. \end{aligned}$$

Using Fubini's theorem and (8) we finally obtain the weak formulation (11). Similarly, we can verify that the entropy condition (6) for \bar{u} implies the entropy condition (12) for u where we use (13). Note that because of (17) the test function $\bar{\varphi}$ is non-negative if and only if φ is non-negative.

Conversely, we assume that u is the entropy solution of the deterministic Cauchy problem (10) and define $\bar{u}(t, x; \omega_\xi) := u(t, x, \omega_\xi)$ for \mathbb{P}_ξ -a.s. $\omega_\xi \in \Omega_\xi$ and for a.e. $x \in \mathbb{R}^d$. We now verify that the weak formulation (11) implies the stochastic weak formulation (5). For this purpose, let be $\bar{\varphi} \in C_0^1([0, T] \times \mathbb{R}^d)$ an arbitrary test function. Furthermore, for $\varepsilon > 0$ let be $J_\varepsilon : \mathbb{R}^m \rightarrow \mathbb{R}$ the rescaled mollifier $J_\varepsilon(\xi) := \frac{1}{\varepsilon^m} J(\xi/\varepsilon)$ with

$$J(\xi) := \begin{cases} c_m \exp\left(\frac{1}{|\xi|^2-1}\right) & , |\xi| < 1 \\ 0 & , |\xi| \geq 1 \end{cases}$$

and $c_m > 0$ chosen such that $\int_{\mathbb{R}^m} J(\xi) d\xi = 1$. By means of the rescaled mollifier we define for fixed $\bar{\xi} \in V$ and $\varepsilon > 0$ chosen such that $B_\varepsilon(\bar{\xi}) \subset V$ the smooth function

$$\varphi(t, x, \xi) := \bar{\varphi}(t, x) J_\varepsilon(\bar{\xi} - \xi) \frac{\chi_V(\Psi^{-1}(\xi))}{|V|} |\det(D_\xi \Psi^{-1})(\xi)|, \quad \xi \in \mathbb{R}^m, \quad (19)$$

where $B_\varepsilon(\bar{\xi})$ is an open ball with radius $\varepsilon > 0$ and center $\bar{\xi} \in V$. Note that the support of φ is bounded because $\text{supp } J_\varepsilon(\bar{\xi} - \cdot) = B_\varepsilon(\bar{\xi})$ and $\text{supp } \varphi \subset \text{supp } \bar{\varphi} \times B_\varepsilon(\bar{\xi}) \subset \text{supp } \bar{\varphi} \times V$. Therefore, it holds $\varphi \in C_0^1([0, T] \times \mathbb{R}^{d+m})$. Then we rewrite (11) applying Fubini's theorem and (9)

$$\begin{aligned} 0 &= \int_{\mathbb{R}^m} \left(\int_0^\infty \int_{\mathbb{R}^d} u(t, x, \xi) \varphi_t(t, x, \xi) + \sum_{j=1}^d f_j(u(t, x, \xi)) \frac{\partial}{\partial x_j} \varphi(t, x, \xi) dx dt \right. \\ &\quad \left. + \int_{\mathbb{R}^d} u_0(x, \xi) \varphi(0, x, \xi) dx \right) d\xi \\ &= \int_{\mathbb{R}^m} \left(\int_0^\infty \int_{\mathbb{R}^d} u(t, x, \xi) \bar{\varphi}_t(t, x) + \sum_{j=1}^d f_j(u(t, x, \xi)) \frac{\partial}{\partial x_j} \bar{\varphi}(t, x) dx dt \right. \\ &\quad \left. + \int_{\mathbb{R}^d} u_0(x, \xi) \bar{\varphi}(0, x) dx \right) J_\varepsilon(\bar{\xi} - \xi) p_\xi(\xi) d\xi. \end{aligned}$$

Since φ has compact support we introduce the weighted residual

$$R(\boldsymbol{\xi}) := \begin{cases} p_{\boldsymbol{\xi}}(\boldsymbol{\xi}) \int_0^{\infty} \int_{\mathbb{R}^d} u(t, x, \boldsymbol{\xi}) \bar{\varphi}_t(t, x) + \sum_{j=1}^d f_j(u(t, x, \boldsymbol{\xi})) \frac{\partial}{\partial x_j} \bar{\varphi}(t, x) dx dt \\ \quad + \int_{\mathbb{R}^d} u_0(x, \boldsymbol{\xi}) \bar{\varphi}(0, x) dx & , \boldsymbol{\xi} \in V \\ 0 & , \boldsymbol{\xi} \in \mathbb{R}^m \setminus V. \end{cases} \quad (20)$$

With the convolution $R_{\varepsilon}(\bar{\boldsymbol{\xi}}) := (J_{\varepsilon} * R)(\bar{\boldsymbol{\xi}})$ it holds $R_{\varepsilon}(\bar{\boldsymbol{\xi}}) \rightarrow R(\bar{\boldsymbol{\xi}})$, $\varepsilon \rightarrow 0$, for a.e. $\bar{\boldsymbol{\xi}} \in V$ leading to $R(\bar{\boldsymbol{\xi}}) = 0$ for a.e. $\bar{\boldsymbol{\xi}} \in V$ and therefore $R(\boldsymbol{\xi}) = 0$ for all $\boldsymbol{\xi} \in \mathbb{R}^m$. Integrating the absolute value of the weighted residual over \mathbb{R}^m we obtain for $\boldsymbol{\xi} = \omega_{\xi}$:

$$\int_{\Omega_{\xi}} \left| \int_0^{\infty} \int_{\mathbb{R}^d} u(t, x, \omega_{\xi}) \bar{\varphi}_t(t, x) + \sum_{j=1}^d f_j(u(t, x, \omega_{\xi})) \frac{\partial}{\partial x_j} \bar{\varphi}(t, x) dx dt \right. \\ \left. + \int_{\mathbb{R}^d} u_0(x, \omega_{\xi}) \bar{\varphi}(0, x) dx \right| d\mathbb{P}_{\xi}(\omega_{\xi}) = 0. \quad (21)$$

This concludes the stochastic weak formulation (5). To verify that the entropy condition (12) implies the stochastic entropy condition (6), we may proceed analogously. \square

We emphasize that in [26,30] it is *not* verified that the entropy solutions of the stochastic Cauchy problem and the deterministic Cauchy problem coincide.

3.2 Existence of the stochastic moments

In general, we are not interested in results of individual realizations of a stochastic problem but in stochastic moments of the solution. The existence of these moments for the stochastic Cauchy problem (4) is proven in [20] assuming higher integrability on the initial conditions. In this section we prove that for the deterministic problem (10) the stochastic moments exist. Since an entropy solution u in the sense of Definition 2 is in $(L^1 \cap L^{\infty})(\mathbb{R}^{d+m})$ we have that $u \in L^k(\mathbb{R}^{d+m})$ for all $k \in \mathbb{N}$ by Hölder's inequality.

Theorem 3 *Let ξ be an absolutely continuous random variable on $(\Omega_{\xi}, \mathcal{F}_{\xi}, \mathbb{P}_{\xi})$ with density $p_{\xi} : \mathbb{R}^m \rightarrow [0, \infty)$. Let u be the entropy solution of (10). Then, for all $t \in [0, T]$ and for all $k \in \mathbb{N}$:*

- (i) $\|\mathbb{E}[u^k(t, \cdot, \cdot)]\|_{L^1(\mathbb{R}^d)} \leq \|u_0\|_{L^k(\mathbb{R}^{d+m})} \|p_{\xi}\|_{L^{\infty}(\mathbb{R}^m)}$
- (ii) $\|\mathbb{E}[u^k(t, \cdot, \cdot)]\|_{L^{\infty}(\mathbb{R}^d)} \leq \|u_0\|_{L^{\infty}(\mathbb{R}^{d+m})}^k$.

Proof (i) Let u be the entropy solution of (10). Since ξ is an absolutely continuous random variable, p_{ξ} is bounded for a.e. $\boldsymbol{\xi} \in \mathbb{R}^m$ and therefore $p_{\xi} \in L^{\infty}(\mathbb{R}^m)$. Since $u_0 \in (L^1 \cap L^{\infty})(\mathbb{R}^{d+m})$ and u is the entropy solution of (10) with $u(t, \cdot, \cdot) \in (L^1 \cap L^{\infty})(\mathbb{R}^{d+m})$ for all $t \in [0, T]$, then it holds $u_0, u(t, \cdot, \cdot) \in L^k(\mathbb{R}^{d+m})$ for all $t \in [0, T]$ and for all $k \in \mathbb{N}$. Thus,

$$\begin{aligned} \|\mathbb{E}[u^k(t, \cdot, \cdot)]\|_{L^1(\mathbb{R}^d)} &\leq \mathbb{E} \left[\|u^k(t, \cdot, \cdot)\|_{L^1(\mathbb{R}^d)} \right] \\ &= \int_{\mathbb{R}^m} \|u(t, \cdot, \boldsymbol{\xi})\|_{L^k(\mathbb{R}^d)}^k p_{\xi}(\boldsymbol{\xi}) d\boldsymbol{\xi} \\ &\leq \|u(t, \cdot, \cdot)\|_{L^k(\mathbb{R}^{d+m})}^k \|p_{\xi}\|_{L^{\infty}(\mathbb{R}^m)} \\ &\leq \|u_0\|_{L^k(\mathbb{R}^{d+m})}^k \|p_{\xi}\|_{L^{\infty}(\mathbb{R}^m)}. \end{aligned}$$

- (ii) The proof is similar and hence omitted. \square

If $u_0 \in (L^1 \cap L^\infty)(\mathbb{R}^{d+m})$, Theorem 3 ensures existence of the stochastic moments. Hence, the expectation exists and it holds

$$\begin{aligned} \mathbb{E}[\|u(t, \cdot, \cdot)\|_{L^1(\mathbb{R}^d)}] &\leq \|u_0\|_{L^1(\mathbb{R}^{d+m})} \|p_\xi\|_{L^\infty(\mathbb{R}^m)}, \\ \mathbb{E}[\|u(t, \cdot, \cdot)\|_{L^\infty(\mathbb{R}^d)}] &\leq \|u_0\|_{L^\infty(\mathbb{R}^{d+m})} \end{aligned} \quad (22)$$

for all $t \in [0, T]$.

4 Approximation of stochastic moments

We are mainly concerned with the approximation of stochastic moments. In the following these moments will be approximated by applying discretization to equation (10). Having a deterministic multi-dimensional hyperbolic (system) conservation law at hand allows to now discretize using modern (adaptive) finite volume or discontinuous Galerkin schemes to equation (10).

To fix the notation, we use the following discretization of the space \mathbb{R}^{d+m} for the variable $y = (x, \xi) \in \mathbb{R}^{d+m}$. Let $\mathcal{I} := \{(i_1, \dots, i_{d+m}) : i_1, \dots, i_{d+m} \in \mathbb{Z}\}$ be a multiindex set and let $\Delta := \{(i_1 \Delta y_1, \dots, i_{d+m} \Delta y_{d+m}) : i \in \mathcal{I}\}$ be the corresponding grid with some fixed grid size $\Delta y := (\Delta y_1, \dots, \Delta y_{d+m})$. A cell $C_{\Delta, i}$ of the grid Δ is given by $C_{\Delta, i} := \prod_{j=1}^{d+m} [(i_j - \frac{1}{2})\Delta y_j, (i_j + \frac{1}{2})\Delta y_j]$ for $i \in \mathcal{I}$. For the temporal discretization of $[0, T]$ we use a uniform discretization $t_n = n\Delta t$ with timestep size $\Delta t > 0$ fulfilling the CFL condition.

Then for any $u \in L^1([0, T] \times \mathbb{R}^{d+m})$ we define the corresponding grid function $u_\Delta = u_\Delta(t, y) := \sum_{i \in \mathcal{I}} u_i^n \chi_{C_{\Delta, i}}(y) \chi_{[t_n, t_{n+1})}(t)$, where $u_i^n := \frac{1}{|C_{\Delta, i}|} \int_{C_{\Delta, i}} u(t_n, y) dy$ is the cell average of u on cell $C_{\Delta, i}$. We assume that the approximation converges to the exact entropy solution u under grid refinement, i.e., for $\Delta t \rightarrow 0$

$$\sup_{t \in [0, T]} \|u_\Delta(t, \cdot, \cdot) - u(t, \cdot, \cdot)\|_{L^1(\mathbb{R}^{d+m})} \rightarrow 0. \quad (23)$$

Furthermore, the approximation is assumed to satisfy a maximum principle

$$\sup_{t \in [0, T]} \|u_\Delta(t, \cdot, \cdot)\|_{L^\infty(\mathbb{R}^{d+m})} \leq \|u_0\|_{L^\infty(\mathbb{R}^{d+m})}. \quad (24)$$

For instance, using a monotone finite volume scheme properties, (23), (24) hold [5, Theorem 1].

By means of this approximation we determine an approximation for the expectation and the centralized moments. We will show that the approximate moments converge to the exact stochastic moments provided the underlying scheme is converging to the entropy solution of (10). The convergence rate of the stochastic moments depends on the convergence rate of the approximation of the entropy solution.

Theorem 4 *Let u_Δ be a converging approximation of the entropy solution u of (10), i.e., (23) holds, with approximate initial data u_Δ^0 . Then for all $t \in [0, T]$ the expectation is bounded by*

$$\|\mathbb{E}[u(t, \cdot, \cdot)] - \mathbb{E}[u_\Delta(t, \cdot, \cdot)]\|_{L^1(\mathbb{R}^d)} \leq \|p_\xi\|_{L^\infty(\mathbb{R}^m)} \|u(t, \cdot, \cdot) - u_\Delta(t, \cdot, \cdot)\|_{L^1(\mathbb{R}^{d+m})}. \quad (25)$$

In addition if we assume that the maximum principle (24) holds for the initial data u_Δ^0 , then for all $k \in \mathbb{N}$ and for all $t \in [0, T]$ the centralized moments fulfill

$$\|\mathcal{M}_c^k[u(t, \cdot, \cdot)] - \mathcal{M}_c^k[u_\Delta(t, \cdot, \cdot)]\|_{L^1(\mathbb{R}^d)} \leq c_k \|u(t, \cdot, \cdot) - u_\Delta(t, \cdot, \cdot)\|_{L^1(\mathbb{R}^{d+m})}, \quad (26)$$

with

$$c_k := \|p_\xi\|_{L^\infty(\mathbb{R}^m)} \sum_{j=0}^k \binom{k}{j} \left((k-j) \|u_0\|_{L^\infty(\mathbb{R}^{d+m})}^{2(k-j)-1} + k \|u_0\|_{L^\infty(\mathbb{R}^{d+m})}^{2k-1} \right). \quad (27)$$

Proof Using linearity of the expectation and an estimate similar to the inequality in the proof of Theorem 3 (i) yields the error bound (25) for the expectation.

To verify the error bound (26) for the k -th centralized moment (2), $k \in \mathbb{N}$, we rewrite these moments using the binomial formula and linearity of the expectation

$$\mathcal{M}_c^k [u(\xi)] = \mathbb{E} \left[\sum_{j=0}^k \binom{k}{j} u^{k-j}(\xi) (-\mathbb{E}[u(\xi)])^j \right] = \sum_{j=0}^k (-1)^j \binom{k}{j} \mathbb{E}[u^{k-j}(\xi)] \mathbb{E}^k [u(\xi)], \quad (28)$$

for some $u \in L^1(\mathbb{R}^m)$. To increase the readability of the proof we drop the arguments of the analytical solution as well as of the grid solutions. Then the left-hand side of (26) can be estimated by

$$\begin{aligned} & \left\| \mathcal{M}_c^k [u] - \mathcal{M}_c^k [u_\Delta] \right\|_{L^1(\mathbb{R}^d)} \\ & \leq \sum_{j=0}^k \binom{k}{j} \left\| \mathbb{E}[u^{k-j}] \mathbb{E}^k [u] - \mathbb{E}[u_\Delta^{k-j}] \mathbb{E}^k [u_\Delta] \right\|_{L^1(\mathbb{R}^d)} \\ & \leq \sum_{j=0}^k \binom{k}{j} \left[\left\| \mathbb{E}^k [u] \right\|_{L^\infty(\mathbb{R}^d)} \left\| \mathbb{E}[u^{k-j}] - \mathbb{E}[u_\Delta^{k-j}] \right\|_{L^1(\mathbb{R}^d)} \right. \\ & \quad \left. + \left\| \mathbb{E}[u_\Delta^{k-j}] \right\|_{L^\infty(\mathbb{R}^d)} \left\| \mathbb{E}^k [u] - \mathbb{E}^k [u_\Delta] \right\|_{L^1(\mathbb{R}^d)} \right]. \end{aligned}$$

To estimate the differences on the right-hand side, note that for all $k \in \mathbb{N}$ and $j = 0, \dots, k-1$ the following inequalities hold

$$\left\| \mathbb{E}[u^{k-j}] - \mathbb{E}[u_\Delta^{k-j}] \right\|_{L^1(\mathbb{R}^d)} \leq \bar{c}_k \|p_\xi\|_{L^\infty(\mathbb{R}^m)} \|u - u_\Delta\|_{L^1(\mathbb{R}^{d+m})}, \quad (29)$$

$$\left\| \mathbb{E}^k [u] - \mathbb{E}^k [u_\Delta] \right\|_{L^1(\mathbb{R}^d)} \leq \tilde{c}_k \|p_\xi\|_{L^\infty(\mathbb{R}^m)} \|u - u_\Delta\|_{L^1(\mathbb{R}^{d+m})} \quad (30)$$

with $\bar{c}_k := (k-j) \|u_0\|_{L^\infty(\mathbb{R}^{d+m})}^{k-j-1}$ and $\tilde{c}_k := k \|u_0\|_{L^\infty(\mathbb{R}^{d+m})}^{k-1}$. To prove these estimates we note that

$$|\alpha^n - \beta^n| \leq n \max\{|\alpha|, |\beta|\}^{n-1} |\alpha - \beta| \quad (31)$$

for $\alpha, \beta \in \mathbb{R}$ and $n \in \mathbb{N}$. Since both the exact solution u as well as the approximated solution u_Δ satisfy the maximum principle (14) and (24), respectively, it holds

$$\left\| \max\{|u|, |u_\Delta|\} \right\|_{L^\infty(\mathbb{R}^{d+m})} \leq \|u_0\|_{L^\infty(\mathbb{R}^{d+m})}. \quad (32)$$

Thus, for all $k \in \mathbb{N}$ and all $j = 0, \dots, k-1$ we can estimate (29) by

$$\begin{aligned} \left\| \mathbb{E}[u^{k-j}] - \mathbb{E}[u_\Delta^{k-j}] \right\|_{L^1(\mathbb{R}^d)} & \leq \|p_\xi\|_{L^\infty(\mathbb{R}^m)} \left\| u^{k-j} - u_\Delta^{k-j} \right\|_{L^1(\mathbb{R}^{d+m})} \\ & \leq \bar{c}_k \|p_\xi\|_{L^\infty(\mathbb{R}^m)} \|u - u_\Delta\|_{L^1(\mathbb{R}^{d+m})} \end{aligned}$$

where we use Theorem 3 (i), Eqns. (31), (32) and Hölder's inequality. Analogously, we verify (30) for all $k \in \mathbb{N}$

$$\left\| \mathbb{E}^k [u] - \mathbb{E}^k [u_\Delta] \right\|_{L^1(\mathbb{R}^d)} \leq \tilde{c}_k \|p_\xi\|_{L^\infty(\mathbb{R}^m)} \|u - u_\Delta\|_{L^1(\mathbb{R}^{d+m})}.$$

Inserting (29) and (30) in (26) yields

$$\begin{aligned} & \left\| \mathcal{M}_c^k [u] - \mathcal{M}_c^k [u_\Delta] \right\|_{L^1(\mathbb{R}^d)} \\ & \leq \|p_\xi\|_{L^\infty(\mathbb{R}^m)} \|u - u_\Delta\|_{L^1(\mathbb{R}^{d+m})} \\ & \quad \times \sum_{j=0}^k \binom{k}{j} \left[\bar{c}_k \left\| \mathbb{E}[u_\Delta^{k-j}] \right\|_{L^\infty(\mathbb{R}^d)} + \tilde{c}_k \left\| \mathbb{E}^k [u] \right\|_{L^\infty(\mathbb{R}^d)} \right]. \end{aligned} \quad (33)$$

Applying Jensen's inequality, (22) and Theorem 3 (ii) we estimate the expectation by the initial data and its approximation

$$\|\mathbb{E}^k[u]\|_{L^\infty(\mathbb{R}^d)} \leq \|u_0\|_{L^\infty(\mathbb{R}^{d+m})}^k, \quad \|\mathbb{E}^{k-j}[u_\Delta]\|_{L^\infty(\mathbb{R}^d)} \leq \|u_\Delta^0\|_{L^\infty(\mathbb{R}^{d+m})}^{k-j}.$$

Then the right-hand side in (33) can be further estimated by

$$\begin{aligned} & \|\mathcal{M}_c^k[u] - \mathcal{M}_c^k[u_\Delta]\|_{L^1(\mathbb{R}^d)} \\ & \leq \|p_\xi\|_{L^\infty(\mathbb{R}^m)} \|u - u_\Delta\|_{L^1(\mathbb{R}^{d+m})} \sum_{j=0}^k \binom{k}{j} \left[\bar{c}_k \|u_\Delta^0\|_{L^\infty(\mathbb{R}^{d+m})}^{k-j} + \tilde{c}_k \|u_0\|_{L^\infty(\mathbb{R}^{d+m})}^k \right] \\ & \leq c_k \|u - u_\Delta\|_{L^1(\mathbb{R}^{d+m})}, \end{aligned}$$

with c_k defined by (27). □

We emphasize that Theorem 4 provides convergence of the moments for the deterministic approach based on the Cauchy problem (10). In contrast to Monte Carlo methods and stochastic Galerkin methods (gPC), the deterministic approach does not depend on the number of samples [20, 19, 1] and the number of terms in the polynomial expansion [33], respectively. Instead, the convergence solely depends on the spatial discretization of the problem (10) which can be seen as collocation points. Therefore, this number can be related to the number of gPC nodes. However, contrary to gPC approaches we do not have spectral convergence. On the other hand there is no requirement to solve for an extended (and possibly) non-hyperbolic system.

Formally, the previous stated approach can be applied also to systems of hyperbolic conservation laws. We will present numerical results for scalar hyperbolic conservation laws as well as for systems of hyperbolic conservation laws in the following section.

5 Numerical results

To investigate the performance of the deterministic approach in comparison to Monte Carlo methods and to verify the theoretical findings in Theorem 4 we perform computations for the different approaches. Here we briefly summarize the methods we are using.

Deterministic solver. For the approximation of a deterministic Cauchy problem we apply a Runge–Kutta discontinuous Galerkin method [4] using polynomial elements of degree $p = 2$ and an explicit third–order SSP–Runge–Kutta method with three stages for the time–discretization. As numerical flux we choose the local Lax–Friedrichs flux with minmod limiter [4]. The performance is enhanced by local multi–resolution based grid adaptation using multiwavelets, see [13]. Details on the adaptive solver can be found in [8, 7]. This solver is applied to approximate both the deterministic Cauchy problem (10) on the higher–dimensional space–stochastic domain as well as to the deterministic Cauchy problem corresponding to the stochastic Cauchy problem (4) for one event when performing Monte Carlo sampling.

Monte Carlo methods. The Monte Carlo (MC) method [33, 16, 20] is a non–intrusive approach to approximate the stochastic moments of a stochastic problem numerically. For this purpose, $N \in \mathbb{N}$ independent, identically distributed realizations of a random variable have to be drawn and for each realization the respective deterministic problem has to be solved numerically. Taking the mean over all those numerical solutions yields an approximation of the expectation (1) of the stochastic Cauchy problem (4). The simple implementation of a MC simulation has a low convergence rate of $\mathcal{O}(N^{-1/2})$ for $N \rightarrow \infty$ [20] and more advanced variations of MC like quasi Monte Carlo (QMC) [29, 21] or randomized quasi Monte Carlo (RQMC) [17] methods have been applied. According to [20], an approximation of the expectation on different levels of resolution of the spatial grid simultaneously leads to the multi–level Monte Carlo (MLMC) method. Thereby, the major part of the realizations can be performed on a coarse grid and just a small number of realizations have to be computed on a fine grid. We use MC, QMC, RQMC and MLMC for comparison in the subsequent section.

Stochastic collocation. To determine the moments in the deterministic problem, we combine multiscale decomposition based on multiwavelets with stochastic collocation [23,28]. To avoid Gibb's phenomenon we use multi-element stochastic collocation [32,10] which performs stochastic collocation separately for each cell of the adaptive grid. In contrast to Monte Carlo simulations or gPC, multiresolution analysis accounts for the local structure of the stochastic by resolving regions with large local changes, such as discontinuities, higher than smooth regions. This leads to an efficient and accurate approximation of the stochastic moments, taking into account the stochasticity of the solution. The number of collocation points on each cell is chosen such that the degree of the resulting polynomial in stochastic collocation corresponds to the degree of the polynomials used in the discontinuous Galerkin scheme.

5.1 Burgers' equation with uncertain initial values

In this example we investigate the one-dimensional Burgers' equation with uncertain initial data. Furthermore, we compare the numerical solutions of our approach with different types of Monte Carlo methods and show the computational effort.

Let $\xi \sim \mathcal{U}(0, 1)$ be a uniform random variable. We consider the one-dimensional stochastic Burgers' equation

$$\partial_t \bar{u}(t, x; \omega_\xi) + \partial_x \left(\frac{\bar{u}^2(t, x; \omega_\xi)}{2} \right) = 0, \quad x \in [-1, 3], \quad t > 0 \quad (34)$$

with different uncertain initial data \bar{u}_r, \bar{u}_s , respectively,

$$\text{a) } \bar{u}_r(0, x; \omega_\xi) = \begin{cases} e^{\omega_\xi} & , x < 0 \\ e & , x > 0 \end{cases}, \quad \text{b) } \bar{u}_s(0, x; \omega_\xi) = \begin{cases} e & , x < 0 \\ e^{\omega_\xi} & , x > 0 \end{cases}. \quad (35)$$

The initial value problem (34), (35) is a Riemann problem with a convex flux function exhibiting an analytical solution for both initial conditions for all realizations ω_ξ of the random variable ξ [18, p. 28ff]. Furthermore, an analytical solution of the expectation and the variance is determined and shown in Figure 1 for time $t = 1.0$. In addition, we present the corresponding 1.0-confidence region of the problems. In the rarefaction case the stochasticity affects the solution up to $x \approx 3$. For the shock case on the other hand, the stochasticity does not affect the solution below $x \approx 2$. To compare the different approaches we measure the L^1 -errors to the analytical solutions of the expectations and of the variance, respectively.

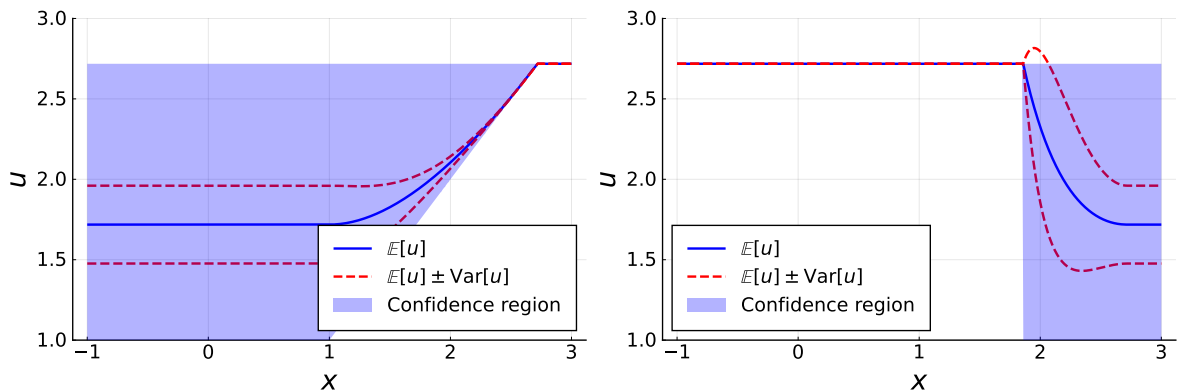


Figure 1: Analytical moments of the one-dimensional Burgers' equation (34) with uncertain initial data (35), corresponding to a rarefaction wave (left) and a shock wave (right) and its 1.0-confidence region.

The deterministic approach (10) corresponding to (34), (35) reads as follows

$$\partial_t u(t, x, \xi) + \partial_x \left(\frac{u^2(t, x, \xi)}{2} \right) = 0, \quad (x, \xi) \in [-1, 3] \times [0, 1], \quad t > 0 \quad (36)$$

with initial condition

$$\text{a) } u_r(0, x, \xi) = \begin{cases} e^\xi, & x < 0 \\ e, & x > 0 \end{cases}, \quad \text{b) } u_s(0, x, \xi) = \begin{cases} e, & x < 0 \\ e^\xi, & x > 0 \end{cases}. \quad (37)$$

Due to the change of the variable we have to consider the space of all possible values of the random variable leading to $\xi \in [0, 1]$. We emphasize that in contrast to the stochastic formulation (4) this formulation treats the stochastic variable as an additional space dimension resulting in a two-dimensional problem. The solution of (36), (37) for the two initial data u_r and u_s are presented in Figure 2. Each

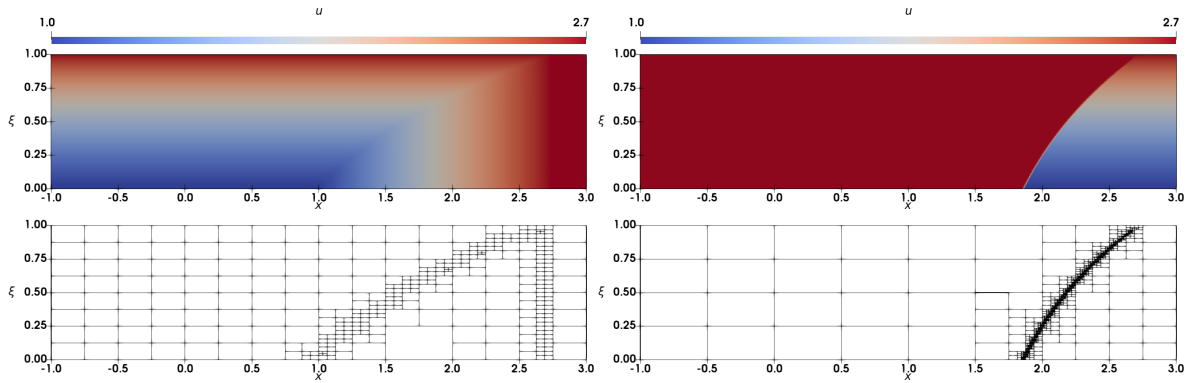


Figure 2: Rarefaction wave (left) and shock wave (right) of the two-dimensional deterministic approach (36), (37) of the Burgers' equation (top row) at time $t = 1.0$ with its adaptive grid (bottom row).

horizontal line represents a realization of a uniform random variable of the original problem (34), (35). Thus, different realizations do not affect each other. For initial data (37a) we obtain for each $\xi \in [0, 1]$ a rarefaction wave, whereby the characteristic speed of the leading and the trailing edge of the rarefaction wave are determined by the value of ξ in the initial condition (37a). On the other hand, for initial data (37b) we observe a shock speed depending on ξ and that the shock travels faster for increasing ξ . In contrast to the rarefaction case, the shock case also has discontinuities in the stochastic direction ξ . Furthermore, we observe that the stochastic influence of our approach is reflected in the confidence regions of the analytical solutions in Figure 1.

On the bottom row of Figure 2 the corresponding adaptive grids via multi-resolution analysis are shown. Obviously, the grids are only refined in locations where the respective solution changes locally, for instance, at the kinks of the rarefaction wave or at the shock. On the other hand, constant regions like the left part of the shock are not refined, allowing to perform the numerical simulations on grids with less cells.

For the numerical simulations we use grids with different refinement levels. For this purpose, let $L \in \mathbb{N}$ be the maximum number of refinement levels, i.e., for each level $\ell = 0, \dots, L$ we have $M_{\ell, x} = 2^\ell M_{0, x}$ cells in x -direction and $M_{\ell, \xi} = 2^\ell M_{0, \xi}$ in ξ -direction, where $M_{0, x}, M_{0, \xi}$ are the number of cells in the initial grid in x -direction or ξ -direction, respectively. In the simulations we have chosen the maximum number of refinement levels $L = 6$ and the number of cells of the initial grid $M_{0, x} = 8$ and $M_{0, \xi} = 4$. We use the same number of cells in x -direction in the simulation of the one-dimensional problem (34) and the two-dimensional approach (36). This ensures to study the stochastic effects on the discretizations of the different methods. To compare the deterministic approach (36), (37) with different Monte Carlo methods, we measure the L^1 -error of the expectation and the L^1 -error of the variance, respectively. For readability, we denote the problems (34) and (36) with initial data (35a)

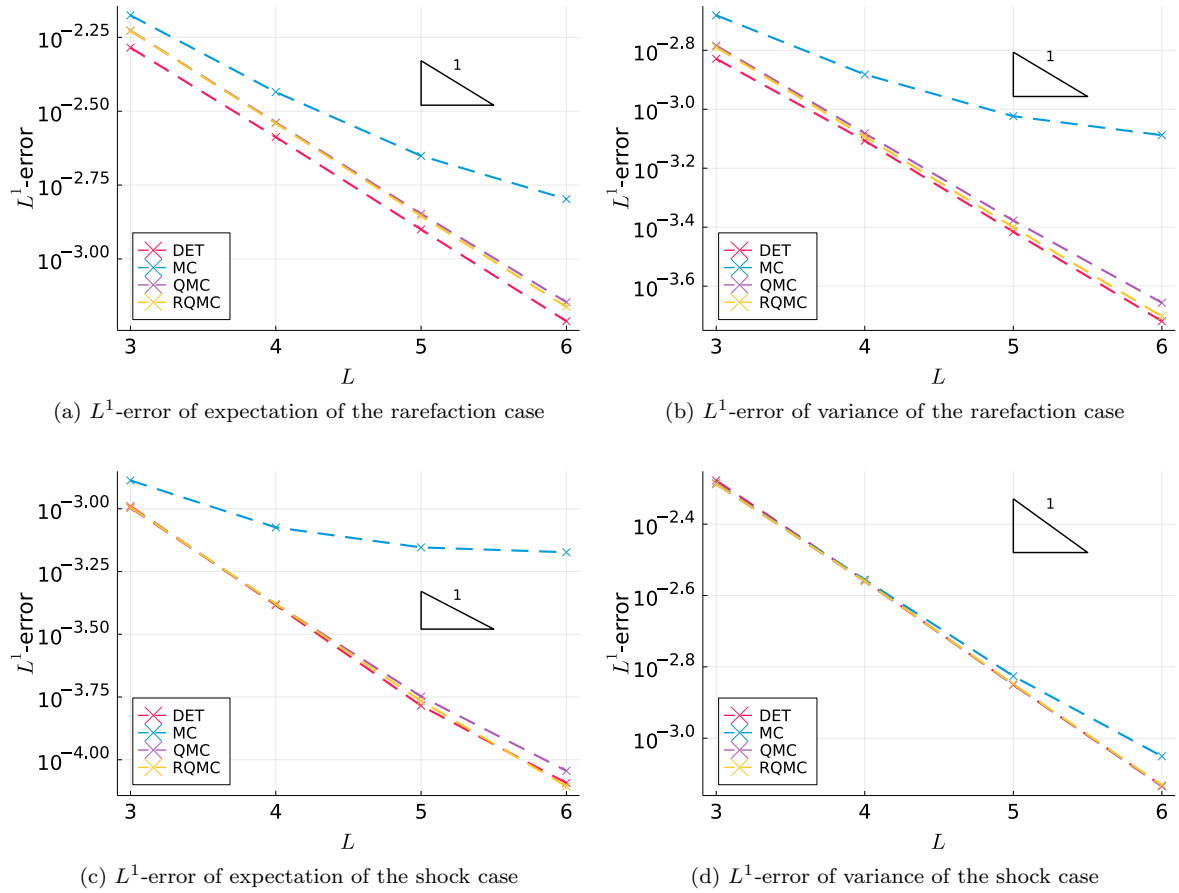


Figure 3: L^1 -error of the moments of the uncertain Burgers' equation at time $t = 1.0$ with $N = 16000$ samples for different Monte Carlo methods and the deterministic approach on an adaptive grid (top row: rarefaction case; bottom row: shock case).

and (37a), respectively, as the rarefaction case and (35b) and (37b) as the shock case, respectively. Figure 3 shows the L^1 -error of the rarefaction case and the shock case using MC, QMC, RQMC and the deterministic approach (DET) on an adaptive grid with different refinement levels. For all Monte Carlo methods we use $N = 16000$ samples on each level. In the rarefaction case MC has a worse convergence rate in comparison to all other approaches. In particular, the error in expectation in the shock case as well as the error in variance using MC is significantly worse than the other approaches. However, the L^1 -error of MC of the variance in the shock case is comparable to all other methods. The methods QMC and RQMC have for all simulations nearly the same convergence rate. On the other hand, our approach has the same behavior as QMC and RQMC and has a slightly better L^1 -error for all simulations. We emphasize that grid adaptation in the deterministic approach also affects the stochastic direction (cf. Figure 2), leading to a coarser resolution of the stochastic space, whereby no refinement strategy in the stochastic can be used in MC, QMC and RQMC methods. We would like to emphasize that our approach benefits from the interplay between the stochastic collocation and multiresolution analysis, which adequately treats the stochasticity of the solution, where Monte Carlo methods are unable to capture high local changes, such as discontinuities, and treat them the same as regions without any stochastic effects.

Since the approach has an additional spatial dimension in the stochastic we investigate the computational effort. To study the performance of the different approaches, we consider the total number of degrees of freedom (DoF) in the approximations and compare those with the related error of the stochastic moments. In contrast to classical comparisons of computational time, for a fair comparison

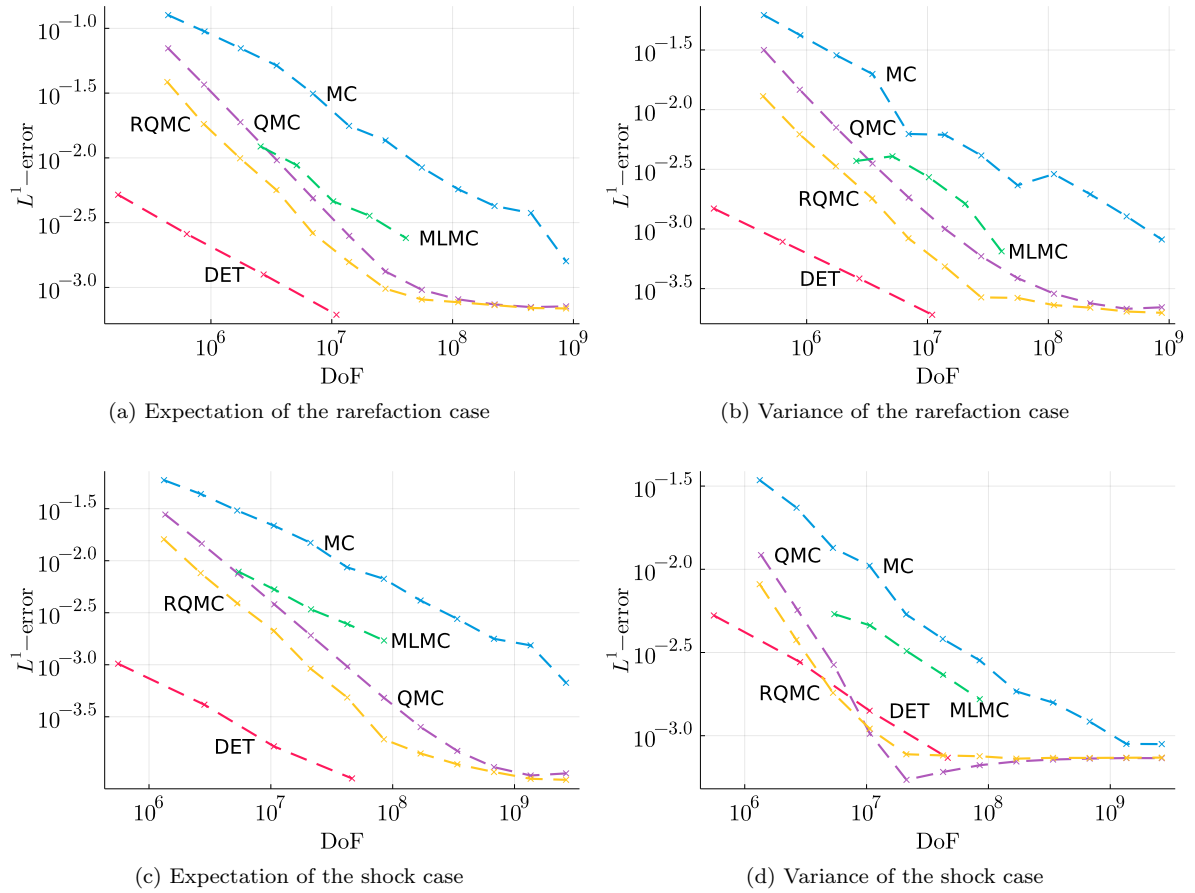


Figure 4: L^1 -error of the moments with respect to the total number of degrees of freedom of the uncertain Burgers' equation at time $t = 1.0$ (top row: rarefaction case, bottom row: shock case).

we investigate the total amount of *all* computations corresponding to the consumed energy over the entire simulation. We note that all Monte Carlo methods are faster than our approach in real time when a large amount of CPU-cores are available due to their perfect scalability capability. Although our higher-dimensional deterministic solver runs in parallel there is some overhead due to load balancing. In contrast to the computational time, the number of the required degrees of freedom of the simulations is proportional to the computation of *all* simulations on a single core. The number of degrees of freedom is obtained by summing up all required degrees of freedom of *all* cells in the adaptive grid over *all* time steps. In contrast to DET, where we need to evaluate the degrees of freedom on a two-dimensional grid, the one-dimensional adaptive grids of the Monte Carlo simulations are different for each realization and therefore need to be considered separately.

In Figure 4 the L^1 -error is shown and the total number of degrees of freedom used in the different algorithms for the rarefaction wave and the shock case, respectively. As before, all calculations are performed on an adaptive grid.

For MC, QMC and RQMC we calculate every experiment on a grid with refinement level $L = 6$ but with different number of samples up to $N = 16000$. To compare the adaptive approaches we also show MLMC. Both, the deterministic approach as well as MLMC are performed on an adaptive grid with different refinement levels up to a maximum refinement level $L = 6$. For MLMC, we use up to $N = 21840$ samples. In the rarefaction case, our approach needs significantly less degrees of freedom to achieve a specific error compared to all Monte Carlo simulations. This is also observed in the error of the expectation in the shock case. Therefore, our approach is more efficient than all other presented methods. Also in the shock case, our approach is able to treat discontinuities in the

stochastic dimension. As before the classical Monte Carlo approach provides the worst result. On the other hand, our approach has no computational advantage over QMC or RQMC in the case of the variance of the shock.

5.2 Burgers' equation with non-uniform uncertain initial values

In this section, we consider the one-dimensional Burgers' equation with uncertain initial data. In contrast to Section 5.1, we consider smooth initial conditions. In addition, we investigate non-uniform random variables. As before, we compare the numerical solutions of our approach with the Monte Carlo method.

To formulate the problem, we first consider ξ to be an absolutely continuous random variable. The stochastic Cauchy problem reads as follows:

$$\partial_t \bar{u}(t, x; \omega_\xi) + \partial_x \left(\frac{\bar{u}^2(t, x; \omega_\xi)}{2} \right) = 0, \quad x \in [0, 1], \quad t > 0 \quad (38)$$

with uncertain initial condition

$$\bar{u}(0, x; \omega_\xi) = \sin(2\pi x) \sin(2\pi \omega_\xi), \quad x \in [0, 1] \quad (39)$$

for all realizations ω_ξ of the random variable ξ . In addition, we assume periodic boundary conditions in the spatial direction. In this section, we consider the following random variables:

$$\xi_1 \sim \mathcal{U}(0, 1), \quad \xi_2 \sim \mathcal{N}(0.5, 0.15), \quad \xi_3 \sim \mathcal{B}(2, 5), \quad \xi_4 \sim \mathcal{B}(5, 2), \quad (40)$$

where $\mathcal{N}(\mu, \sigma^2)$ is the normal distribution with mean $\mu \in \mathbb{R}$ and variance $\sigma^2 > 0$ and $\mathcal{B}(\alpha, \beta)$ is the beta distribution for $\alpha, \beta > -1$.

To reformulate the stochastic Cauchy problem (38), (39) in our deterministic formulation we have to define the space of all possible outcomes of the random variables (40). Since the density of the uniform random variable ξ_1 and the densities of the beta distributed random variables ξ_3, ξ_4 have compact support in $[0, 1]$, we choose $\boldsymbol{\xi} \in [0, 1]$. Since the density of the normal distribution ξ_2 has non-compact support, we have to cutoff the domain for the numerical simulations. In this case, choosing $\boldsymbol{\xi} \in [0, 1]$ guarantees that more than 99.9% of all realizations are taken into account. Thus, the deterministic approach of problem (38), (39) for the random variables ξ_1, \dots, ξ_4 reads

$$\partial_t u(t, x, \boldsymbol{\xi}) + \partial_x \left(\frac{u^2(t, x, \boldsymbol{\xi})}{2} \right) = 0, \quad (x, \boldsymbol{\xi}) \in [0, 1] \times [0, 1], \quad t > 0 \quad (41)$$

with uncertain initial condition

$$u(0, x, \boldsymbol{\xi}) = \sin(2\pi x) \sin(2\pi \boldsymbol{\xi}), \quad (x, \boldsymbol{\xi}) \in [0, 1] \times [0, 1] \quad (42)$$

and periodic boundary conditions in the spatial direction of x . The numerical solution of (41), (42) is presented in Figure 5.

As before, we interpret each horizontal line as a realization of the corresponding random variable. For $\boldsymbol{\xi} < 0.5$ a stationary shock is located at $x = 0.5$, whereby for $\boldsymbol{\xi} > 0.5$ there is a rarefaction wave. Due to the periodic boundary conditions, the roles are reversed at the boundaries $x = 0$ and $x = 1$. Thus, for $\boldsymbol{\xi} < 0.5$ a rarefaction wave develops at the boundaries whereby for $\boldsymbol{\xi} > 0.5$ a stationary shock occurs. In addition, we apply grid adaptation via multi-resolution analysis. The corresponding adaptive grid is also shown in Figure 5. Obviously, the grid is more refined in regions with large local changes and less refined in regions with smooth data.

To evaluate the stochastic moments, we apply multi-element stochastic collocation. We emphasize that we have to calculate the numerical solution of (41), (42) only once for all random variables ξ_1, \dots, ξ_4 in (40). The stochastic moments of these problems are then computed in a post-processing step where we have to adjust the evaluation of the solution for each random variable. We refer to [32, 10] for more details.

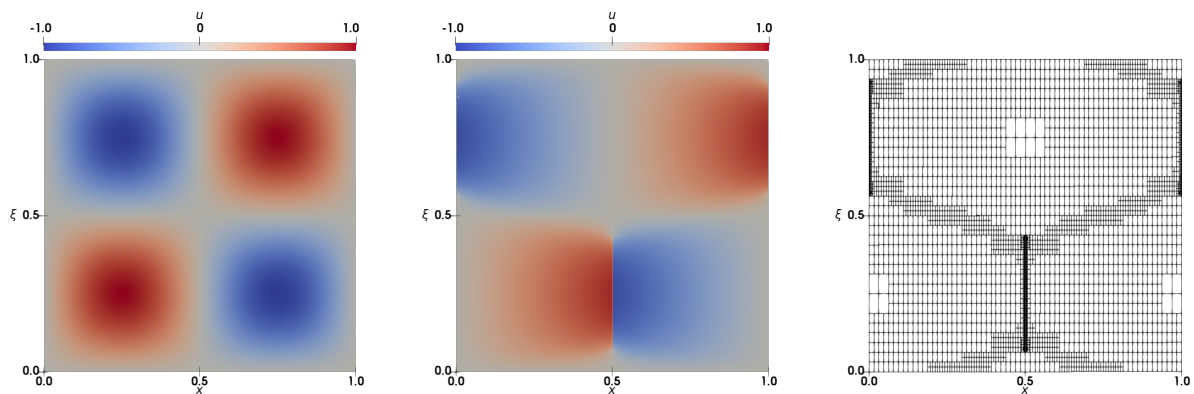


Figure 5: Solution for the Burgers' equation (41) with uncertain initial data (42). Left: Initial data at time $t = 0$; Middle: Numerical solution at time $t = 0.35$; Right: Corresponding adaptive grid for the numerical solution at time $t = 0.35$.

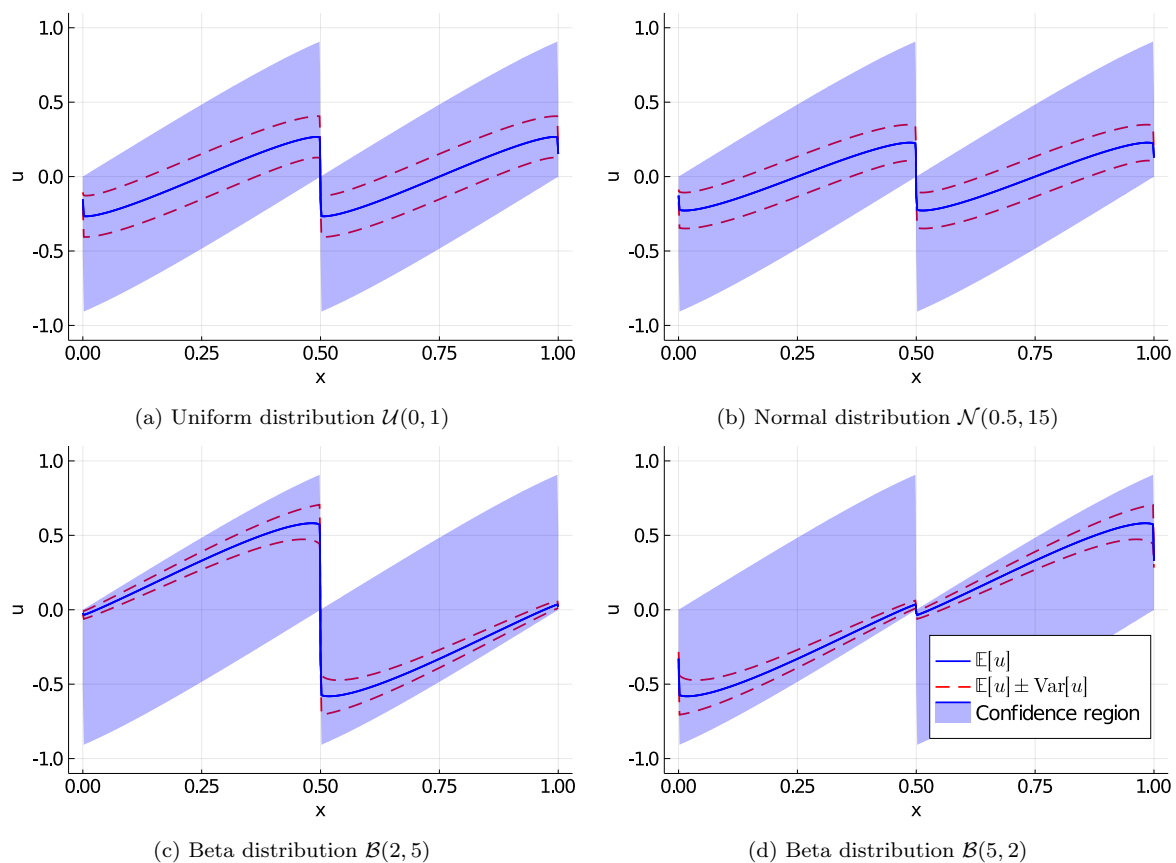


Figure 6: Stochastic moments of the problem (41), (42) for the different random variables (40) at time $t = 0.35$.

The stochastic moments obtained by our deterministic approach (41), (42) for all random variables (40) are shown in Figure 6. The uniform distributed random variable ξ_1 and the normal distributed random variable ξ_2 behave similar due to the symmetry of the corresponding densities at $\xi = 0.5$. Since the mass of the normal distributed random variable ξ_2 is more concentrated around $\xi = 0.5$ than the mass of the uniform distribution, the variance of the normal distributed random variable ξ_2 is slightly smaller than the variance of the uniform random variable ξ_1 . In contrast to this, the mass of the beta distributed random variables ξ_3 and ξ_4 is more concentrated in the regions $\xi < 0.5$ and $\xi > 0.5$, respectively. For example, for the random variable ξ_3 , where the region $\xi < 0.5$ is preferred, the effects of the stationary shock at $x = 0.5$ dominate the stochastic moments. On the other hand, for the random variable ξ_4 , where most drawn realizations are in the region $\xi > 0.5$, the rarefaction wave at $x = 0.5$ dominates the stochastic moments, with small influence of the stationary shock. Due to the periodic boundary conditions, these effects are reversed at the boundary, respectively. In addition, in Figure 6 we show the confidence interval of our approach to illustrate the affected regions of the different random variables.

Next, we verify that the numerical approximation of the stochastic moments using our approach is comparable to Monte Carlo simulations. In particular, we show that our approach has a better performance in terms of the total number of degrees of freedom used during the simulations. As described in Section 5.1 we use an adaptive grid with increasing refinement levels. In the simulations we choose the maximum number of refinement level $L = 6$ and we set the number of cells in the initial grid to $M_{0,x} = 8$ in the spatial direction and $M_{0,\xi} = 16$ in the stochastic direction for the deterministic approach. As before, we fix the number of cells $M_{0,x}$ in the initial grid for all Monte Carlo simulations. In Figure 7, we compare the L^1 -error of the expectation and the variance of the different approaches with the corresponding stochastic moments of a reference solution with respect to the total number of degrees of freedom. Here the reference solution is computed on a uniform mesh with $L = 11$ refinement levels. As before, we refer to Section 5.1 for more information. For the deterministic approach we use an adaptive grid with maximum refinement level $L = 3, \dots, 6$, as described above, whereby all Monte Carlo simulations are performed on an adaptive grid with refinement level $L = 6$ and with varying number of samples up to $N = 16000$.

In Figures 7 (a), (b) we see that for the uniform random variable ξ_1 our method is much more efficient than the Monte Carlo method, especially in approximating the expectation. For the normal distributed random variable ξ_2 , our approach is still more efficient than the Monte Carlo simulation, although our approach is no longer as efficient as in the uniform case, see Figures 7 (c), (d). The same behavior is also observed for the beta distributed random variable ξ_3 in Figures 7 (e), (f). Nevertheless, our approach has a higher performance in approximating the stochastic moments but does not reach the efficiency of the uniform case. Because of the periodic boundary conditions and because of the symmetry of ξ_4 with respect to ξ_3 at $\xi = 0.5$, the L^1 -error of the beta distribution ξ_4 behaves almost the same as the L^1 -error of ξ_3 and is therefore omitted in Figure 7.

The worse efficiency of the approximation of non-uniform random variables can be justified by the fact that the adaptive grid of the numerical solutions of (41), (42) is the same for all random variable (40). Thus, the grid adaptation treats all regions equally regardless of the local stochastic behavior. Although, this adaptation strategy provides a good efficient approximation of the moments, it is not optimal for non-uniform random variables. The investigation of an adaptation strategy with respect to the stochastic behavior will be part of future work.

5.3 Euler equations with uncertain initial conditions

Here, we consider the one-dimensional Euler equations for a perfect gas with uncertain initial data. Especially, we investigate Sod's shock tube problem [27] and assume uncertain initial pressure on the left. For this purpose, let be $\xi \sim \mathcal{U}(0.2, 1.0)$ a random variable. We define for a realization ω_ξ the conserved variable $\bar{\mathbf{u}}(t, x; \omega_\xi) := (\bar{\rho}, \bar{\rho}\bar{v}, \bar{\rho}\bar{E})^T$ describing the conservation of mass, momentum and energy. Here, $\bar{\rho} \equiv \bar{\rho}(t, x; \omega_\xi)$, $\bar{v} \equiv \bar{v}(t, x; \omega_\xi)$ and $\bar{E} \equiv \bar{E}(t, x; \omega_\xi)$ denote density, momentum and total

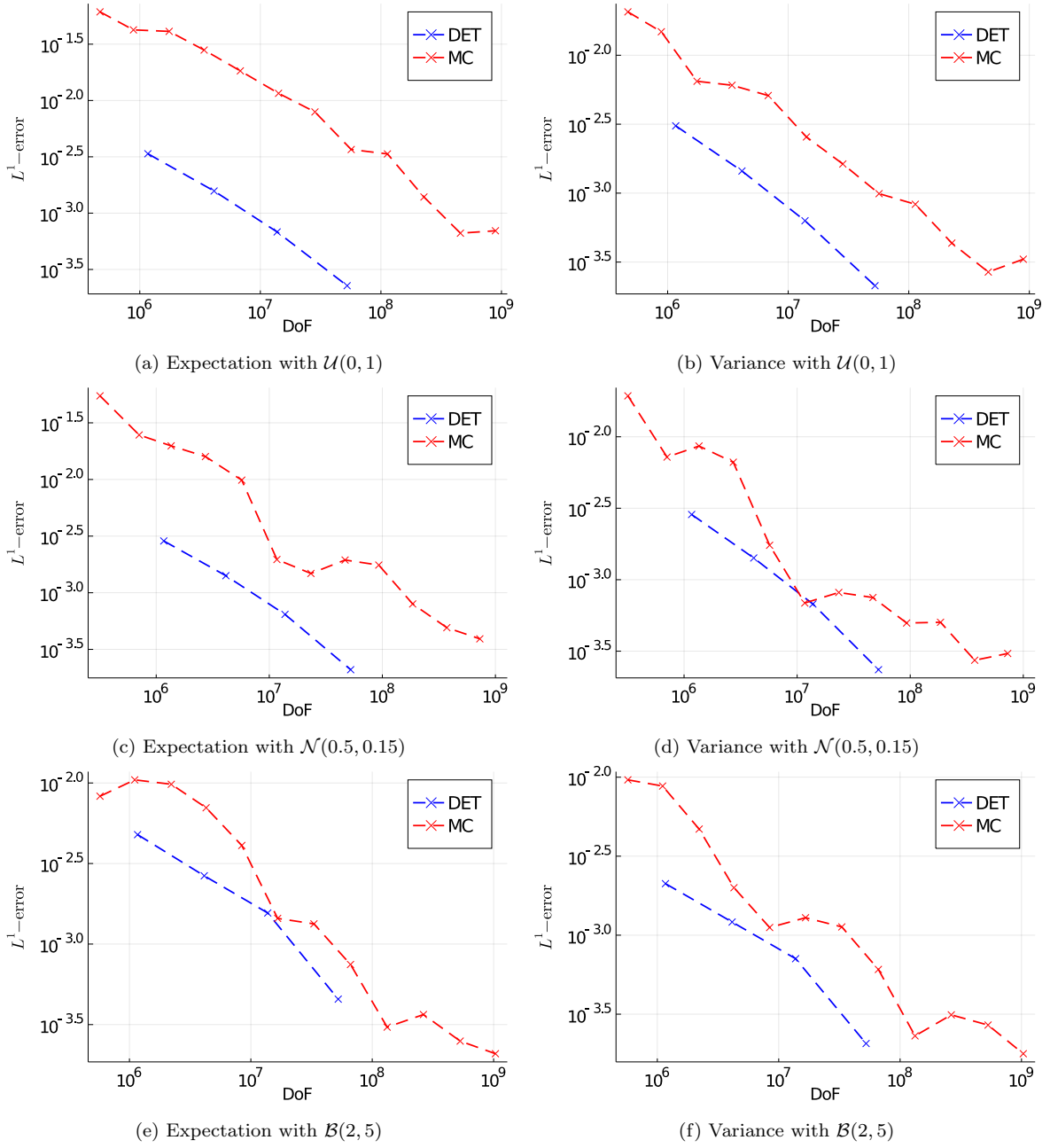


Figure 7: L^1 -error of the moments with respect to the total number of degrees of freedom of the Cauchy problem with uncertain initial data at time $t = 0.35$.

energy, respectively, with

$$\bar{E} = \frac{1}{2}\bar{v}^2 + \bar{e}, \quad (43)$$

where $\bar{e} \equiv \bar{e}(t, x; \omega_\xi)$ is the internal energy of the system. We consider a perfect gas

$$\bar{e} = \frac{\bar{p}}{(\gamma - 1)\bar{\rho}} \quad (44)$$

with $\gamma = 1.4$ [31]. We investigate the behavior of the system with uncertain initial pressure on the left

$$\bar{p}(0, x; \omega_\xi) = \begin{cases} \omega_\xi, & x \leq 0.5 \\ 0.1, & x > 0.5 \end{cases}. \quad (45)$$

The Euler equations are then

$$\partial_t \bar{\rho} + \partial_x(\bar{\rho} \bar{v}) = 0, \quad (46a)$$

$$\partial_t(\bar{\rho} \bar{v}) + \partial_x(\bar{\rho} \bar{v}^2 + \bar{p}) = 0, \quad x \in \mathbb{R}, t > 0, \quad (46b)$$

$$\partial_t(\bar{\rho} \bar{E}) + \partial_x(\bar{v}(\bar{\rho} \bar{E} + \bar{p})) = 0. \quad (46c)$$

and the corresponding uncertain initial data is

$$\bar{\mathbf{u}}(0, x; \omega_\xi) = \begin{cases} (1.0, 0.0, 2.5\omega_\xi)^T, & x \leq 0.5 \\ (0.125, 0.0, 0.2)^T, & x > 0.5 \end{cases}. \quad (47)$$

The initial value (47) is constructed such that for all realizations ω_ξ the pressure on the left side is always higher than the pressure on the right side. This allows us to investigate the behavior of the Sod's shock tube.

We replace the stochastic parameter ω_ξ at the expense of an additional space dimension. Therefore, the conserved variable becomes $\mathbf{u}(t, x, \boldsymbol{\xi}) := (\rho, \rho v, \rho E)^T$ for $(x, \boldsymbol{\xi}) \in \mathbb{R} \times [0.2, 1.0]$, where $\rho \equiv \rho(t, x, \boldsymbol{\xi})$, $v \equiv v(t, x, \boldsymbol{\xi})$, $E \equiv E(t, x, \boldsymbol{\xi})$ and $p \equiv p(t, x, \boldsymbol{\xi})$. The initial condition of the pressure is given by

$$p(0, x, \boldsymbol{\xi}) = \begin{cases} \boldsymbol{\xi}, & x \leq 0.5 \\ 0.1, & x > 0.5 \end{cases}. \quad (48)$$

Thus, the deterministic approach of the system (46) reads

$$\partial_t \rho + \partial_x(\rho v) = 0, \quad (49a)$$

$$\partial_t(\rho v) + \partial_x(\rho v^2 + p) = 0, \quad (x, \boldsymbol{\xi}) \in \mathbb{R} \times [0.2, 1.0], t > 0, \quad (49b)$$

$$\partial_t(\rho E) + \partial_x(v(\rho E + p)) = 0, \quad (49c)$$

with initial condition

$$\mathbf{u}(0, x, \boldsymbol{\xi}) = \begin{cases} (1.0, 0.0, 2.5\boldsymbol{\xi})^T, & x \leq 0.5 \\ (0.125, 0.0, 0.2)^T, & x > 0.5 \end{cases}. \quad (50)$$

The solution to (49), (50) for the final time $t = 0.2$ is presented in Figure 8. Each horizontal cut represents the solution of a single realization of the problem (49), (50). We observe that for higher initial pressure the shock wave, the contact wave and the rarefaction wave propagate faster. This leads to discontinuities in the new (stochastic) direction for the leading shock wave. On the other hand, we only observe discontinuities for the conserved variables $(\rho, \rho v, \rho E)^T$ in the new direction across the contact discontinuity with no discontinuities for velocity v and pressure p . Thus, the solution only exhibits discontinuities in the new direction when there are discontinuities in the spatial direction, too. Furthermore, we perform a multiresolution analysis which triggers finer grid resolution in non-smooth areas and smooth regions are resolved on a coarser grid. The resulting adaptive grid is shown in Figure 8.

To verify our approach, we compare the stochastic moments of our approach with the stochastic moments obtained by Monte Carlo simulation of the one-dimensional problem (46), (47). For both approaches the initial grid has $M_{0,x} = 4$ cells in x -direction. Additionally, we set the number of cells in $\boldsymbol{\xi}$ -direction to $M_{0,\boldsymbol{\xi}} = 4$. The maximum number of refinement levels is set to $L = 6$ for both simulations. For the Monte Carlo simulations we fix the number of samples to $N = 32000$. The comparison is presented in Figure 9 at the final time $t = 0.2$. The expectations of both methods nearly coincide, whereby the variance differs slightly. To investigate the total range of all possible realizations we show the corresponding 1.0-confidence region of the our approach containing \mathbb{P} -almost all realizations of the problem. The confidence regions are also reflected in Figure 8 describing the stochastic influence on each component.

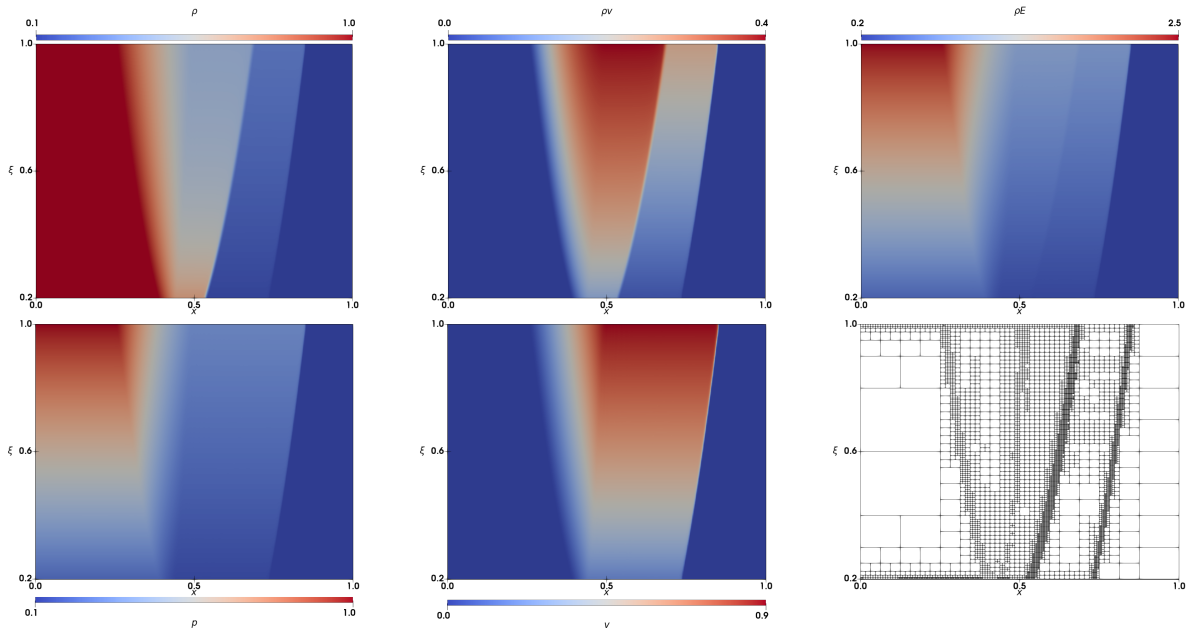


Figure 8: Solution for the uncertain Euler equations at time $t = 0.2$. Top row (from left to right): density ρ ; momentum ρv ; density of energy ρE . Bottom row (from left to right): pressure p ; velocity v ; adaptive grid.

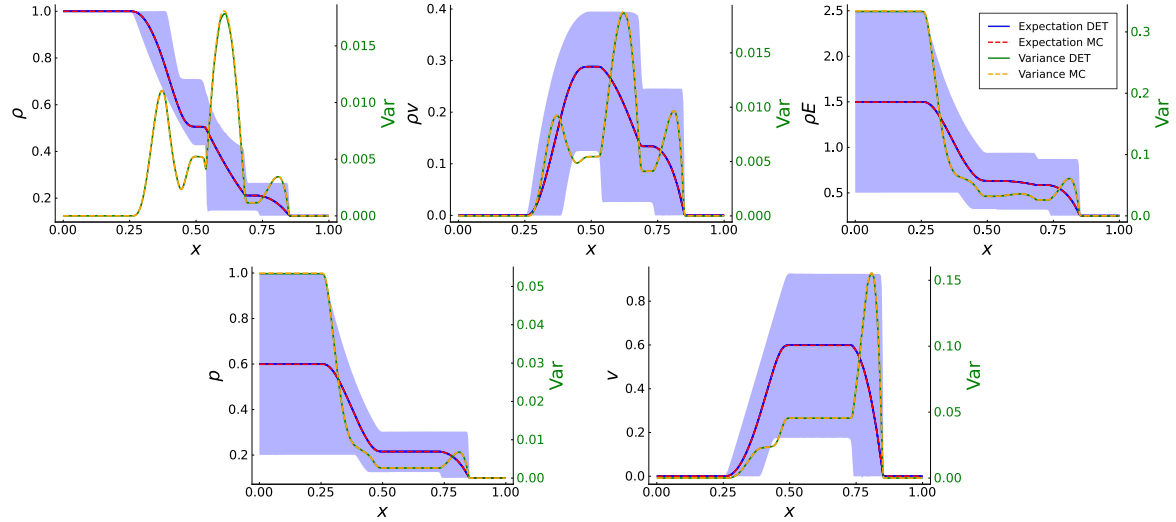


Figure 9: Comparison of stochastic moments between our approach and a Monte Carlo simulation together with its 1.0-confidence region at time $t = 0.2$. Top row (from left to right): density ρ ; momentum ρv ; density of energy ρE . Bottom row (from left to right): pressure p ; velocity v .

6 Conclusion

A deterministic approach to determine stochastic moments for scalar problems and systems of hyperbolic conservation laws with uncertain initial data has been presented. The idea is to interpret stochastic variables of the original problem as additional spatial dimensions with zero flux. For this approach we have proven that the entropy solution of our approach coincides with the random entropy solution [20]. Furthermore, we have shown the existence of stochastic moments as well as numerical

convergence of approximate stochastic moments. Our theoretical results have been verified numerically with two experiments for Burgers' equation and the Euler equations for both uniform and non-uniform random variables.

It turned out that applying an adaptive discretization in space and stochastic simultaneously improves the efficient computation of the stochastic moments in comparison to Monte-Carlo-type methods. In particular, the efficiency improves if the uncertain solution exhibits discontinuities in the stochastic variable. Compared to gPC approaches the proposed method does not require to deal with possibly non-hyperbolic formulations. The presented approach allows us to study the interplay between the spatial scales and the stochastic scales of the solution. On this basis, an improved adaptation strategy can be considered which is subject of ongoing research.

References

1. Badwaik, J., Klingenberg, C., Risebro, N.H., Ruf, A.M.: Multilevel Monte Carlo finite volume methods for random conservation laws with discontinuous flux. *ESAIM: Mathematical Modelling and Numerical Analysis* **55**(3), 1039–1065 (2021). DOI 10.1051/m2an/2021011
2. Bauer, H.: *Measure and Integration Theory*. DE GRUYTER (2001). DOI 10.1515/9783110866209
3. Cameron, R.H., Martin, W.T.: The orthogonal development of non-linear functionals in series of Fourier-Hermite functionals. *The Annals of Mathematics* **48**(2), 385 (1947). DOI 10.2307/1969178
4. Cockburn, B., Shu, C.W.: The Runge-Kutta discontinuous Galerkin method for conservation laws V: Multidimensional systems. *J. Comput. Phys.* **141**, 199–244 (1998)
5. Crandall, M.G., Majda, A.: Monotone difference approximations for scalar conservation laws. *Mathematics of Computation* **34**(149) (1980). DOI 10.1090/s0025-5718-1980-0551288-3
6. Dürrwächter, J., Kuhn, T., Meyer, F., Schlachter, L., Schneider, F.: A hyperbolicity-preserving discontinuous stochastic Galerkin scheme for uncertain hyperbolic systems of equations (2018). DOI 10.1016/j.cam.2019.112602
7. Gerhard, N., Iacono, F., May, G., Müller, S., Schäfer, R.: A high-order discontinuous Galerkin discretization with multiwavelet-based grid adaptation for compressible flows. *J. Sci. Comput.* **62**(1), 25–52 (2015). DOI 10.1007/s10915-014-9846-9
8. Gerhard, N., Müller, S.: Adaptive multiresolution discontinuous Galerkin schemes for conservation laws: multi-dimensional case. *Comp. Appl. Math.* **35**(2), 321–349 (2016). DOI 10.1007/s40314-014-0134-y
9. Ghanem, R.: *Stochastic Finite Elements: A Spectral Approach*. Springer New York, New York, NY (1991)
10. Giesselmann, J., Meyer, F., Rohde, C.: A posteriori error analysis and adaptive non-intrusive numerical schemes for systems of random conservation laws. *BIT Numerical Mathematics* **60**(3), 619–649 (2020). DOI 10.1007/s10543-019-00794-z
11. Godlewski, E., Raviart, P.A.: *Hyperbolic systems of conservation laws*. Paris: Ellipses-Edition Marketing (1991)
12. Gottlieb, D., Xiu, D.: Galerkin method for wave equations with uncertain coefficients. *Communications in Computational Physics* **3**, 505–518 (2008)
13. Hovhannisyan, N., Müller, S., Schäfer, R.: Adaptive multiresolution discontinuous Galerkin schemes for conservation laws. *Math. Comput.* **83**(285), 113–151 (2014)
14. Hu, J., Jin, S.: A stochastic Galerkin method for the Boltzmann equation with uncertainty. *Journal of Computational Physics* **315**, 150–168 (2016). DOI 10.1016/j.jcp.2016.03.047
15. Kadry, S.: On the theory of stochastic transformation method **702**, 304–309 (2013). DOI 10.4028/www.scientific.net/amr.702.304
16. Le Maître, O.P., Knio, O.M.: *Spectral Methods for Uncertainty Quantification*. Springer-Verlag GmbH (2010)
17. L'Ecuyer, P., Lemieux, C.: Recent advances in randomized quasi-Monte Carlo methods. In: *International Series in Operations Research & Management Science*, pp. 419–474. Springer US (2002). DOI 10.1007/0-306-48102-2_20
18. Leveque, R.J.: *Numerical Methods for Conservation Laws*. Birkhäuser Basel (2008)
19. Mishra, S., Risebro, N.H., Schwab, C., Tokareva, S.: Numerical solution of scalar conservation laws with random flux functions. *SIAM/ASA Journal on Uncertainty Quantification* **4**(1), 552–591 (2016). DOI 10.1137/120896967
20. Mishra, S., Schwab, C.: Sparse tensor multi-level Monte Carlo finite volume methods for hyperbolic conservation laws with random initial data. *Mathematics of Computation* **81**(280), 1979–2018 (2012). DOI 10.1090/s0025-5718-2012-02574-9
21. Niederreiter, H.: *Random number generation and quasi-Monte Carlo methods*. Society for Industrial and Applied Mathematics, Philadelphia (1992)
22. Nordström, J.: Conservative finite difference formulations, variable coefficients, energy estimates and artificial dissipation. *Journal of Scientific Computing* **29**(3), 375–404 (2005). DOI 10.1007/s10915-005-9013-4
23. Nordström, J., Iaccarino, G., Pettersson, M.P.: *Polynomial Chaos Methods of Hyperbolic Partial Differential Equations*. Springer-Verlag GmbH (2015)
24. Öfner, P., Glaubit, J., Ranocha, H.: Stability of correction procedure via reconstruction with summation-by-parts operators for Burgers' equation using a polynomial chaos approach. *ESAIM: Mathematical Modelling and Numerical Analysis* **52**(6), 2215–2245 (2018). DOI 10.1051/m2an/2018072
25. Pulch, R., Xiu, D.: Generalised polynomial chaos for a class of linear conservation laws. *Journal of Scientific Computing* **51**(2), 293–312 (2011). DOI 10.1007/s10915-011-9511-5

26. Schwab, C., Tokareva, S.: High order approximation of probabilistic shock profiles in hyperbolic conservation laws with uncertain initial data. *ESAIM: Mathematical Modelling and Numerical Analysis* **47**(3), 807–835 (2013). DOI 10.1051/m2an/2012060
27. Sod, G.A.: A survey of several finite difference methods for systems of nonlinear hyperbolic conservation laws. *Journal of Computational Physics* **27**(1), 1–31 (1978). DOI 10.1016/0021-9991(78)90023-2
28. Sullivan, T.J.: *Introduction to Uncertainty Quantification*. Springer-Verlag GmbH (2016)
29. Taimre Botev, K.: *Handbook of Monte Carlo Methods*. John Wiley and Sons (2011)
30. Tokareva, S.: *Stochastic finite volume methods for computational uncertainty quantification in hyperbolic conservation laws*. Ph.D. thesis (2013). DOI 10.3929/ETHZ-A-009965237
31. Toro, E.F.: *Riemann Solvers and Numerical Methods for Fluid Dynamics*. Springer-Verlag GmbH (2009)
32. Wan, X., Karniadakis, G.E.: Multi-element generalized polynomial chaos for arbitrary probability measures. *SIAM Journal on Scientific Computing* **28**(3), 901–928 (2006). DOI 10.1137/050627630
33. Xiu, D.: *Numerical methods for stochastic computations: a spectral method approach*. Princeton University Press, Princeton, N.J (2010)
34. Xiu, D., Karniadakis, G.E.: The Wiener–Askey polynomial chaos for stochastic differential equations. *SIAM Journal on Scientific Computing* **24**(2), 619–644 (2002). DOI 10.1137/s1064827501387826
35. Zanella, M.: Structure preserving stochastic Galerkin methods for Fokker–Planck equations with background interactions. *Mathematics and Computers in Simulation* **168**, 28–47 (2020). DOI 10.1016/j.matcom.2019.07.012

Declarations

Funding

Funded by the Deutsche Forschungsgemeinschaft (DFG, German Research Foundation) – project number 320021702/GRK2326–Energy, Entropy and Dissipative Dynamics and by DFG HE5386/18-1,19-1,22-1 and 333849990/IRTG-2379.

Conflicts of interest/Competing interests

There are no conflicts of interest.

Availability of data and material

Data will be made available on reasonable request.

Code availability

Code will not be made available.